Hydraulic Conductivity of Geosynthetic Clay Liners to Low-Level Radioactive Waste Leachate

Kuo Tian, A.M.ASCE[1]; Craig H. Benson, F.ASCE[2]; and William J. Likos, M.ASCE[3]

Abstract: Hydraulic conductivity was evaluated for eight commercially available geosynthetic clay liners (GCLs) permeated with leachate characteristic of low-level radioactive waste (LLW) disposal facilities operated by the U.S. Department of Energy (DOE). Two of the GCLs (CS and GS) contained conventional sodium bentonite (Na-B). The others contained a bentonite–polymer mixture (CPL, CPH, GPL1, GPL2, and GPH) or bentonite–polymer composite (BPC). All GCLs (except GPL2 and GPH) were permeated directly with two synthetic LLW leachates that are essentially identical, except one has no radionuclides (nonradioactive synthetic leachate, or NSL) and the other has radionuclides (radioactive synthetic leachate, or RSL). Hydraulic conductivities to RSL and NSL were identical. For the CS and GS GCLs, the hydraulic conductivity gradually increased by a factor of 5–25 because divalent cations in the leachate replaced native sodium cations bound to the bentonite. The CPL, GPL1, and GPL2 GCLs with low polymer loading (1.2–3.3%) had hydraulic conductivities similar to the conventional GCLs. In contrast, hydraulic conductivity of the CPH, GPH, and BPC GCLs with high polymer loading (≥5%) to RSL or NSL was comparable to, or lower than, the hydraulic conductivity to deionized water. Permeation with leachate reduced the swell index of the bentonite in all of the GCLs. A conceptual model featuring pore blocking by polymer hydrogel is proposed to explain why the hydraulic conductivity of bentonite–polymer GCLs to LLW leachates remains low even though the leachate inhibits bentonite swelling. **DOI: 10.1061/(ASCE)GT.1943-5606.0001495.**

Author keywords: Geosynthetic clay liner; Bentonite; Low-level radioactive waste; Polymer; Hydrogel.

Introduction

Geosynthetic clay liners (GCLs) are factory-manufactured hydraulic barriers consisting of a thin layer of sodium bentonite (Na-B) clay (approximately 3–5 kg/m^2) sandwiched between two geotextiles that are bonded by needle punching or stitching (Shackelford et al. 2000). Some GCLs also include a geomembrane bonded to the bentonite, or laminated to the geotextile. GCLs are common elements in waste containment facilities due to their low hydraulic conductivity to water (typically $< 10^{-10}$ m/s) and ease of installation (Shackelford et al. 2000; Jo et al. 2001, 2005; Kolstad et al. 2004a; Benson et al. 2010), including composite liners for low-level radioactive waste (LLW) and mixed waste (MW) disposal facilities (e.g., Powell et al. 2011).

The effectiveness of conventional GCLs is controlled primarily by the hydraulic conductivity of the Na-B in the GCL, which is predominately composed of the clay mineral montmorillonite (Shan and Daniel 1991; Shackelford et al. 2000; Jo et al. 2001, 2005; Lee and Shackelford 2005; Kolstad et al. 2004a; Bradshaw and Benson 2014; Tian and Benson 2014). Osmotic swelling of montmorillonite yields narrow and tortuous flow channels, resulting in low hydraulic conductivity (Mesri and Olson 1971; Jo et al. 2001; Kolstad et al. 2004a; Scalia et al. 2014). However, chemical interactions between Na-B and waste leachates can limit osmotic swelling and result in higher hydraulic conductivity. GCLs permeated with aggressive leachates having high ionic strength or a predominance of polyvalent cations can be orders of magnitude more permeable than GCLs permeated with deionized (DI) or tap water (Petrov and Rowe 1997; Ruhl and Daniel 1997; Shackelford et al. 2000; Jo et al. 2001, 2005; Vasko et al. 2001; Egloffstein 2002; Kolstad et al. 2004a; Benson et al. 2010; Scalia et al. 2014). GCLs containing polymer-modified bentonites have been proposed for applications where leachates affect Na-B adversely (Onikata et al. 1996, 1999; Trauger and Darlington 2000; Ashmawy et al. 2002; Kolstad et al. 2004b; Katsumi et al. 2008; Di Emidio et al. 2010; Scalia et al. 2014).

Hydraulic conductivity of GCLs to municipal solid waste (MSW) leachate has been studied by Petrov and Rowe (1997), Ruhl and Daniel (1997), Guyonnet et al. (2009), and Bradshaw and Benson (2014). Studies with real MSW leachate show minimal impact on hydraulic conductivity of GCLs (<6 × increase relative to DI water) because MSW leachates typically have modest ionic strength (typical = 80 mM) and monovalent cations (Na^+ and NH_4^+) are predominant (Bradshaw and Benson 2014). In contrast, low-level radioactive waste leachates have an abundance of divalent cations (e.g., Ca^{2+} and Mg^{2+}), are more dilute than MSW leachates, and contain radionuclides. Consequently, the hydraulic conductivity of GCLs to LLW leachate cannot be inferred from past studies using MSW leachates. Quantifying the hydraulic conductivity of GCLs to LLW leachates is necessary for conducting the analyses required for performance-based design of LLW and MW disposal facilities.

Hydraulic conductivity of eight commercially available GCLs to synthetic LLW leachate was evaluated in this study. Two were

[1]Postdoctoral Research Associate, Dept. of Civil and Environmental Engineering, Univ. of Virginia, Charlottesville, VA 22904 (corresponding author). E-mail: kt5bk@virginia.edu

[2]Dean, School of Engineering and Applied Science, Univ. of Virginia, Charlottesville, VA 22904. E-mail: chbenson@virginia.edu

[3]Professor, Dept. of Civil and Environmental Engineering, Geological Engineering, Univ. of Wisconsin-Madison, Madison, WI 53706. E-mail: likos@wisc.edu

Note. This manuscript was submitted on September 8, 2015; approved on January 8, 2016; published online on April 25, 2016. Discussion period open until September 25, 2016; separate discussions must be submitted for individual papers. This paper is part of the ***Journal of Geotechnical and Geoenvironmental Engineering***, © ASCE, ISSN 1090-0241.

conventional GCLs containing Na-B (CS and GS) and six GCLs contained bentonite–polymer (B-P) mixtures (CPL, CPH, GPL1, GPL2, and GPH) or a bentonite–polymer composite (BPC). Five of the six B-P GCLs were prepared by dry mixing Na-B and proprietary polymers; the sixth contained a mixture comprised of 90% Na-B and 10% of the bentonite–polymer composite described in Scalia et al. (2014). The GCLs were permeated with two synthetic leachates—radioactive synthetic leachate (RSL) and a nonradioactive synthetic leachate (NSL)—representative of LLW leachates encountered in lined on-site disposal facilities operated by the U.S. Department of Energy (Tian 2012). NSL was chemically identical to RSL, but without radionuclides. Comparative tests were conducted with RSL and NSL to determine if radionuclides in LLW leachate affect bentonite adversely, a heretofore unresolved issue of significant importance when conducting performance assessments for LLW disposal facilities.

Background

Effect of Permeant Solution on Swelling and Hydraulic Conductivity

Hydraulic conductivity is inversely related to swelling of the bentonite in conventional GCLs (Jo et al. 2001; Kolstad et al. 2004a; Meer and Benson 2007; Scalia and Benson 2011). Water molecules associated with swelling of bentonite are tightly bound to the mineral surface and are immobile relative to water molecules in the bulk pore water (Mesri and Olson 1971; Kolstad et al. 2004a; Meer and Benson 2007; Scalia and Benson 2011). Consequently, as swelling occurs, larger pores between bentonite granules are filled with mineral solid and tightly bound water molecules, which results in narrower and more tortuous flow paths in which mobile water flows, and low hydraulic conductivity. Conversely, flows paths between bentonite granules are larger and less tortuous if swelling is suppressed, resulting in higher hydraulic conductivity.

Swelling of bentonite occurs primarily in the interlayer of montmorillonite, which is the predominant mineral in bentonite. Interlayer swelling of montmorillonite occurs in two phases: the crystalline phase and the osmotic phase (Norrish and Quirk 1954; Jo et al. 2001; Kolstad et al. 2004a; Meer and Benson 2007; Bouazza and Bowders 2010; Scalia and Benson 2011; Scalia et al. 2014). During crystalline swelling, up to four discrete layers of water molecules associate with the mineral surface and the bound cations. Osmotic swelling occurs subsequent to crystalline swelling as water molecules migrate into the interlayer in response to a gradient in osmotic head between the bulk pore water and the interlayer pore water (Norrish and Quirk 1954). Crystalline swelling occurs regardless of cation valence in the exchange complex, whereas osmotic swelling occurs only when monovalent cations are predominant in the exchange complex. The magnitude of osmotic swelling is inversely proportional to the concentration of cations in the pore water (Norrish and Quirk 1954). For these reasons, permeant solutions that are predominantly divalent or have high ionic strength suppress osmotic swelling, resulting in GCLs with higher hydraulic conductivity (Jo et al. 2001, 2005; Kolstad et al. 2004a; Meer and Benson 2007; Scalia and Benson 2011).

Jo et al. (2001, 2005) and Kolstad et al. (2004a) demonstrate that ionic strength, relative abundance of monovalent and polyvalent cations, and pH of the permeant solution are master variables affecting osmotic swelling and the hydraulic conductivity of bentonite in GCLs containing Na-B. Kolstad et al. (2004a) quantify the relative abundance of monovalent and polyvalent cations using the parameter RMD

$$\text{RMD} = \frac{M_m}{\sqrt{M_d}} \tag{1}$$

where M_m = total molar concentration of monovalent cations and M_d = total molar concentration of polyvalent cations. For a given ionic strength, GCLs permeated with solutions having low RMD (i.e., polyvalent cations predominant in permeant solution) have higher hydraulic conductivity (Kolstad et al. 2004a).

pH can also be important because high proton concentrations at very low pH elevate ionic strength, suppressing osmotic swell. Dissolution of the mineral at high or low pH can also release multivalent cations that suppress osmotic swell (Jo et al. 2001).

Composition of LLW Leachates in DOE Disposal Facilities

Tian (2012) analyzed leachate data from four disposal facilities operated by the U.S. Department of Energy and identified a synthetic LLW leachate for testing barrier materials. Tian (2012) reports that LLW leachate in DOE disposal facilities predominantly contains inorganic macrocomponents, but also contains trace heavy metals and radionuclides. The major cations are Ca^{2+} (0.77–24.9 mM), Mg^{2+} (0.20–30.2 mM), Na^{+} (0.19–38.13 mM), and K^{+} (0.04–1.94 mM), and the major anions are SO_4^{2-} (0.39–29.6 mM) and Cl^{-} (0.12–19.3 mM). The predominant radionuclides in leachates from DOE facilities are uranium (6.4–3,060 μg/L), tritium (40–4,625 Bq/L), and technetium-99 (0.3–47.8 Bq/L).

Ionic strength and RMD of LLW leachates from DOE facilities are shown in Fig. 1 along with data for MSW leachates from Bradshaw and Benson (2014). DOE LLW leachates typically have lower ionic strength than MSW leachate, and leachates from some facilities have lower RMD. Divalent cations (e.g., Ca^{2+} and Mg^{2+}) in the LLW leachate are responsible for the lower RMD. Tian (2012) indicates that LLW leachates have greater abundance of divalent cations because contaminated soil and demolition debris (e.g., concrete) are a predominant waste stream at DOE disposal facilities and portland cement grouts are often used to solidify waste forms prior to disposal.

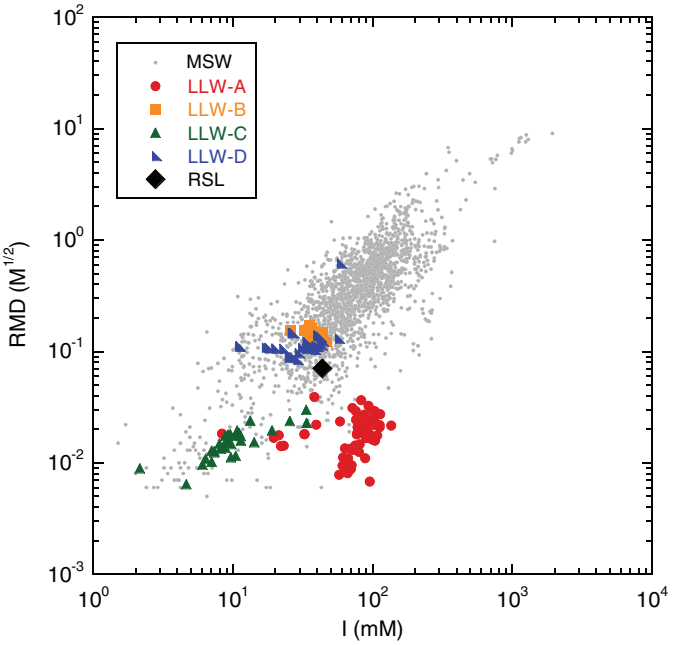

Fig. 1. (Color) RMD versus ionic strength for LLW and MSW leachates. RSL is shown as a solid black diamond. A, B, C, and D designate four DOE disposal facilities used to characterize LLW leachate

Table 1. Characteristics of Radioactive Synthetic Leachate (RSL) Used in This Study

Group	Components	Quantity	Unit
Major cation concentrations	Ca^{2+}	4	mM
	Mg^{2+}	6	mM
	Na^{+}	7	mM
	K^{+}	0.7	mM
Major anion concentrations	SO_4^{2-}	7.5	mM
	Cl^{-}	8	mM
	NO_3^{-}	1.5	mM
	HCO_3^{-}	3.5	mM
Trace metal concentrations	As	0.001	mM
	Ba	0.002	mM
	Cu	0.0002	mM
	Fe	0.04	mM
	Li	0.02	mM
	Al	0.03	mM
	Mn	0.01	mM
	Ni	0.0003	mM
	Sr	0.02	mM
	Zn	0.0005	mM
Radionuclide concentrations	U-238	1,500	μg/L
	H-3	4,440	Bq/L
	Tc-99	29.6	Bq/L
Bulk characteristics	TOC	8	mg/L
	Eh	120	mV
	pH	7.2	—
	Ionic strength	43.6	mM
	RMD	0.077	$M^{1/2}$

Tian (2012) created the synthetic LLW leachate summarized in Table 1 to represent the leachates observed in DOE LLW facilities. The synthetic LLW leachate includes major cations (e.g., Ca^{2+}, Mg^{2+}, K^{+}, and Na^{+}), major anions (e.g., Cl^{-} and SO_4^{2-}), trace metals (e.g., Al, Cu, and Fe), and radionuclides (e.g., ^{238}U, ^{99}Tc, and tritium). Average concentrations in the database were assigned to each constituent, except for radionuclides, which were set at upper-bound concentrations to represent worst-case conditions (Tian 2012). The pH (approximately 7.2) and Eh (approximately 120 mV) of the LLW leachate were also set at the averages in the LLW leachate database.

Bentonite–Polymer Mixtures and Composites

Bentonites have been blended with polymers or organic molecules as a means to prevent or reduce adverse chemical interactions with permeant solutions. For example, Onikata et al. (1996, 1999) intercalated large organic molecules within the interlayer of montmorillonite to enhance swelling in solutions with higher ionic strength. Scalia et al. (2014) found that polymers in a bentonite–polymer composite clogged intergranular flow paths, thereby reducing the hydraulic conductivity even in highly aggressive solutions. Trauger and Darlington (2000) proffered that polymers can prevent or reduce cation exchange in bentonite, but resistance to exchange has not been demonstrated experimentally.

Onikata et al. (1996, 1999) and Katsumi et al. (2008) created multiswellable bentonite (MSB) by intercalating propylene carbonate (PC) molecules in the interlayer of montmorillonite to enhance swelling of Na-B in aggressive leachates. Onikata et al. (1996) report osmotic swelling of MSB in NaCl solutions having an ionic strength of up to 750 mM, whereas osmotic swell in conventional Na-B is limited to ionic strengths < 300 mM (Norrish and Quirk 1954). Katsumi et al. (2008) evaluated the long-term hydraulic conductivity of MSB with 25% PC to NaCl solutions. For concentrations < 1,000 mM, the hydraulic conductivity to the NaCl solution was approximately the same as the hydraulic conductivity to DI water (approximately 10^{-11} m/s) (Katsumi et al. 2008), whereas the hydraulic conductivity of conventional Na-B was approximately two orders of magnitude higher when the NaCl concentration exceeded 500 mM. MSB also had low hydraulic conductivity (approximately 10^{-11} m/s) when permeated with 50 to 500 mM $CaCl_2$, whereas the hydraulic conductivity of conventional GCLs with Na-B to these $CaCl_2$ solutions is orders of magnitude higher (approximately 10^{-8} m/s) (Jo et al. 2001).

Scalia et al. (2014) evaluated GCLs containing a bentonite–polymer composite created by in situ polymerization of acrylic acid with bentonite. The BPC had low hydraulic conductivity ($<8 \times 10^{-11}$ m/s) to a broad range of aggressive inorganic leachates (200 mM CaCl2, 500 mM CaCl2, 1 M NaOH, or 1 M HNO3) to which GCLs with conventional Na-B are very permeable ($>10^{-7}$ m/s). Scalia et al. (2014) hypothesized that BPC had low hydraulic conductivity because polymers that detached from the montmorillonite clogged intergranular flow paths that would be responsible for high hydraulic conductivity in conventional Na-B.

Some B-P GCLs may not be compatible with aggressive leachates. For example, Shackelford et al. (2010) conducted hydraulic conductivity tests on GCLs containing a *contaminant-resistant* polymer-modified bentonite using synthetic process water and acidic leachate from a mine waste disposal facility. GCLs containing the *contaminant-resistant* B-P were 2,300–7,600 times more permeable to synthetic process water or acidic leachate than to site groundwater. Thus, leachate-specific testing can be necessary to confirm that B-P GCLs are resistant to a particular chemical solution.

Materials and Methods

Geosynthetic Clay Liner

Eight commercially available GCLs were evaluated in this study. Two of the GCLs contained conventional Na-B (CS and GS) and six contained B-P mixtures (CPL, CPH, GPL1, GPL2, GPH, and BPC). The CPL, CPH, GPL1, GPL2, and GPH GCLs contained a dry mixture of granular bentonite and a proprietary polymer, whereas the BPC GCL used a blend of 90% Na-B and 10% of the bentonite–polymer composite created using the slurry polymerization process described by Scalia et al. (2014). The first letter (C or G) in the GCL designation specifies the GCL source. The middle letter in the designations for the B-P GCLs refers to "polymer." The last letter in the designations refers to polymer loading [L = low (<5%), H = high (≥5%)]. Each GCL consisted of granular material (bentonite granules, mixture of bentonite and polymer granules, or granules of BPC) sandwiched between nonwoven (top) and woven polypropylene (bottom) geotextiles bonded by needle punching. Properties of the GCLs are summarized in Table 2. Polymer contents and polymer types were not provided by the GCL manufacturers.

The major mineral components in both the conventional Na-B and the B-P mixtures were determined by X-ray diffraction on the bulk material using the methods described by Scalia et al. (2014), and are summarized in Table 3. Montmorillonite is the predominant mineral in the Na-B and the B-P mixtures. Quartz, plagioclase, feldspar, oligoclase, illite, mica, and calcite are present in measureable quantities, and trace amounts of other minerals (orthoclase, siderite, clinoptilolite, and kaolinite) are also present. The bentonites have similar mineralogy even though the GCLs were obtained from different manufacturers. Granule size distributions for the bentonites are shown in Fig. 2 following ASTM D422 (ASTM

Table 2. Mass per Area, Polymer Loading, Swell Index, Concentrations of Bound Cations in the Exchange Complex, and CEC of Bentonite or Bentonite–Polymer Mixture in GCLs

GCL	Dry mass per area (kg/m^2)	LOI (%)	Polymer loading (%)	Swell index in DI water (mL/2 g)	Mole fraction of bound cations				CEC (cmol$^+$/kg)
					Na^+	K^+	Ca^{2+}	Mg^{2+}	
CS	3.6	1.6	—	36	0.45	0.04	0.29	0.12	71.3
GS	3.7	1.6	—	32	0.42	0.03	0.31	0.10	73.2
CPL	3.6	2.8	1.2	28	0.53	0.03	0.25	0.11	71.4
GPL1	3.7	3.5	1.9	28	0.57	0.02	0.33	0.04	72.1
GPL2	3.7	4.8	3.3	31	0.40	0.02	0.37	0.09	74.6
CPH	3.6	6.6	5.1	27	0.14	0.01	0.13	0.04	89.6
GPH	3.7	12.3	10.9	40	0.46	0.02	0.35	0.15	72.2
BPC	4.8	11.0	12.7	45	0.75	0.01	0.09	0.04	91.5

Note: Polymer loading is calculated based on loss on ignition per ASTM D7348 (ASTM 2013). Swell index measured in DI water using ASTM D5890. Bound cations and CEC measured using ASTM D7503 (ASTM 2010). "—" indicates not available or not applicable.

Table 3. Mineralogy of Bentonite in GCLs

Mineral	Relative abundance (%)							
	CS	GS	CPL	GPL1	GPL2	CPH	GPH	BPC
Montmorillonite	84	86	86	80	85	79	67	78
Quartz	9	8	8	6	10	8	13	8
Plagioclase, feldspar, and oligoclase	3	3	3	9	2	7	9	5
Illite and mica	1	—	1	trc	1	1	7	7
Calcite	1	—	trc	trc	trc	—	3	—
Other minerals	2	3	2	5	2	5	1	2

Note: "—" indicates not available or applicable; trc = trace amount.

2007). Bentonite from the GS, GPL1, and GPL2 GCLs have a relatively uniform distribution of fine sand-size granules, and the bentonites from CS, CPL, CPH, and BPC GCLs have a relatively uniform distribution of medium sand-size granules. The GPH GCL has a similar granule size distribution as the CS GCL for granular sizes larger than 0.42 mm, and a granule size distribution close to the GS GCL for granule sizes smaller than 0.25 mm.

Loss on ignition (LOI) determined via ASTM D7348 (ASTM 2013) was used as an indicator of polymer loading in the bentonite, as suggested by Scalia et al. (2014). Polymer loading was calculated assuming that the polymer additives only contained organic compounds that are combusted completely during the LOI test and by discounting the LOI of the conventional Na-B. The LOI of both conventional Na bentonites was 1.6%, which is attributed to loss of strongly bound water molecules (Grim 1968), decomposition of calcite, and combustion of any organic matter in the bentonite. The CPL, GPL1, and GPL2 GCLs had low polymer loading (<5%), whereas the CPH, GPH, and BPC GCLs had high polymer loading (≥5%) (Table 2).

Mole fractions of the bound cations (BC) and the cation exchange capacity (CEC) for each bentonite measured using the procedure in ASTM D7503 (ASTM 2010) are provided in Table 2. Na^+ is the predominant cation in the exchange complex of all of the bentonites prior to permeation except for the CPH GCL. BPC has a very high mole fraction of Na^+ because a sodic solution is used to manufacture this composite material (Scalia et al. 2014). The mole fraction of Na in the BC of the CPH GCL was much lower than expected, but was confirmed by duplicate tests. The polymer used in this GCL may have affected the extraction used in ASTM D7503 (ASTM 2010), leading to the low Na mole fraction. The effect of polymers on extractions made using ASTM D7503 (ASTM 2010) is being explored.

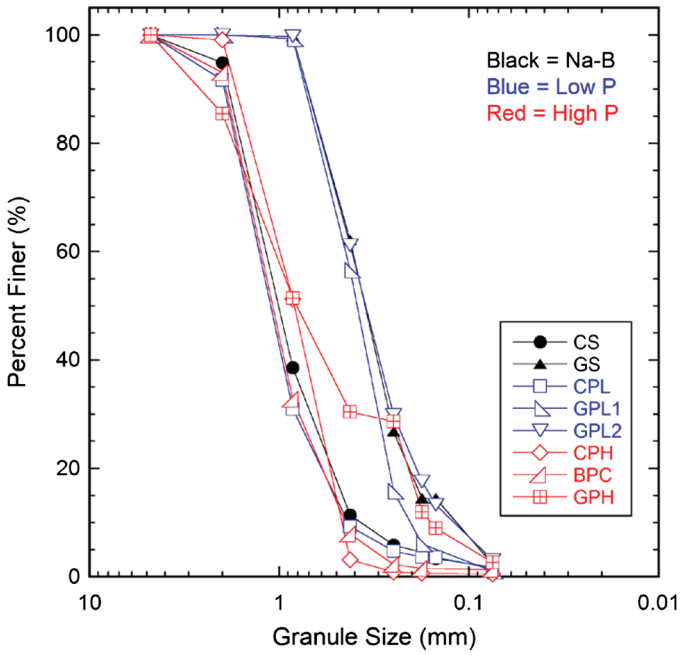

Fig. 2. (Color) Granule size distribution of bentonites in GCLs used in this study (P = polymer loading)

Swell indices of the bentonites in DI water measured using the procedure in ASTM D5890 (ASTM 2006b) are provided in Table 2. Swell indices of the B-P mixtures with low or modest polymer loading (e.g., CPL, GPL1, GPL2, and CPH) are comparable to the swell indices of conventional Na-B, whereas the bentonites with high polymer loading (GPH and BPC) have much higher swell indices due to swelling of the polymer additives.

Permeant Liquids

RSL, NSL, and DI water were used as permeant liquids. The constituents of RSL and NSL are summarized in Table 1. As indicated previously, the RSL and NSL are based on an analysis of leachate data from LLW disposal facilities operated by the U.S. Department of Energy (Tian 2012). NSL has the same chemical composition as RSL, but has no radionuclides.

The RSL and NSL solutions were prepared by mixing $CaCl_2$, $MgSO_4$, $NaNO_3$, $NaHCO_3$, Na_2SO_4, and $KHCO_3$ in Type II DI water per ASTM D1193 (ASTM 2006a). Trace metal components

were added as sulfur salts of Al, Fe, Mn, Zn, Ni, and Cu and chloride salts of Li and Ba. A standard solution used for analytical calibration was used as the source of As (1,000 mg/L As in 2% nitric acid). ^{238}U was added to the synthetic leachate as uranyl acetate [$UO_2(CH_3COO)_2 \cdot 2H_2O$], ^{99}Tc as sodium pertechnetate ($NaTcO_4$), and tritium as water molecules. Major cation and anion concentrations were adjusted to ensure charge balance and to prevent precipitation.

The ionic strength and RMD of RSL are shown in Fig. 1. Trace elements and radionuclides in the RSL and NSL account for less than 1% of the ionic strength; radionuclides contribute to ionic strength and RMD by less than 0.03%. Thus, NSL plots at essentially the same location as RSL in Fig. 1.

Hydraulic Conductivity Testing

Hydraulic conductivity of the GCL specimens was measured in flexible-wall permeameters using the falling headwater and constant tailwater method described in ASTM D6766 (ASTM 2012). The GCLs were hydrated with permeant liquid in the permeameter at an effective confining stress of 10 kPa for 48 h, with the effluent line closed. After hydration, the effective confining stress was increased to 20 kPa, and the average hydraulic gradient was set at approximately 130. Influent was contained in 50-mL burettes sealed with parafilm to prevent evaporation. Effluent was collected in 60-mL polyethylene bottles sealed with parafilm. One specimen each of CS, GS, CPL, GPL2, CPH, and BPC GCL was permeated with RSL and NSL. The GPL1 and GPH GCLs, which were tested later, were permeated with only NSL. Control tests were conducted on all of the GCLs with DI water as the permeant liquid.

Termination Criteria

The hydraulic and chemical termination criteria in ASTM D6766 (ASTM 2012) were applied to all tests. The hydraulic termination criteria in D6766 require no temporal trend in the hydraulic conductivity measurements, hydraulic conductivity falling within 25% of the mean for three consecutive measurements, incremental effluent volume (Q_{out}) within 25% of the incremental influent volume (Q_{in}) for at least three measurements, and the ratio Q_{out}/Q_{in} exhibiting no temporal trend. The chemical termination criteria require no temporal trend in electrical conductivity of the effluent (EC_{out}) and that EC_{out} falls within 10% of the electrical conductivity of the influent (EC_{in}). In addition to the criteria in D6766, pH of the effluent (pH_{out}) was also required to have no temporal trend and to fall within 10% of the pH of the influent (pH_{in}). Concentrations of major cations in influent and effluent were required to have no temporal trend and to be within 10%.

Chemical Analysis

Concentrations of major cations (Ca^{2+}, Mg^{2+}, K^+, and Na^+) in the influent and effluent were analyzed periodically for elemental concentrations by inductively coupled plasma-optical emission spectroscopy (ICP-OES) using U.S. EPA Method 6010C (U.S. EPA 2007). Prior to analysis, the influent and effluent samples were filtered through a 0.2-μm filter, preserved with 1% nitric acid, and stored at 4°C. All analytical and quality control procedures followed USEPA SW-846 for inorganic analytes.

Microscale Imaging Analysis

The spatial distribution and structure of the polymer in the B-P was examined using images obtained using a scanning electron microscope (SEM, LEO 1550 Gemini ZEISS, Jena, Germany). Saturated B-P mixtures were freeze-dried using liquid nitrogen prior to imaging to minimize disturbance of the clay fabric, polymer structure, and clay–polymer interactions established under saturated conditions. Rapid cooling in liquid nitrogen prevents crystallization of water molecules and the associated volume change that occurs during transition from the liquid to solid phase (Nireesha et al. 2013), inhibiting breakdown of the polymer structure. Drying under vacuum at low temperature (−75°C) allows the ice to sublimate directly from solid to vapor in pores previously occupied by liquid (Annabi et al. 2010).

After permeation, each B-P GCL specimen was gently removed from the permeameter. The top geotextile on each GCL was removed using a surgical knife and the remaining specimen was trimmed into 10×30 mm strips. The B-P strips were frozen in liquid nitrogen and transferred to a benchtop freeze-dry system (Labconco-7740020 Kansas City, Missouri) for drying. After freeze-drying, the B-P strips were cut into thin pieces and coated with gold for 30 s using a sputtering system (Denton vacuum Desk II, Moorestown, New Jersey).

Results and Discussion

Table 4 summarizes results of the hydraulic conductivity tests. The pore volumes of flow (PVF) reported in Table 4 are based on the initial pore volume of each GCL before permeation. At the time this paper was prepared, the GCLs had been permeated for up to 2.8 years with RSL and NSL. The CS, GS, CPL, GPL1, and GPL2 GCLs permeated with RSL or NSL met all of the termination criteria in ASTM D6766 (ASTM 2012), and the supplemental criteria regarding pH and the concentrations of major cations in the influent and effluent. The CPH, GPH, and BPC GCLs permeated with RSL or NSL had not met all of the termination criteria because of their very low hydraulic conductivity. Computations based on the current data suggest that these tests will require at least another 5 years of permeation to reach chemical equilibrium. Tests on these GCLs are still ongoing.

Temporal Behavior and Chemical Analysis

Typical data from a hydraulic conductivity test are shown in Fig. 3 for the GS GCL. The hydraulic conductivity increases by approximately a factor of 10 during the initial 40 PVF due to cation exchange processes [Fig. 3(a)]. At approximately 40 PVF, the EC and pH of the effluent level off and fall within the range associated with the EC and pH termination criteria [Fig. 3(b)]. However, the hydraulic conductivity continues to increase very slowly until 80 PVF, which reflects slow rate-limited cation exchange processes, as described by Jo et al. (2001, 2006). Similar behavior was observed for all other GCLs for which the hydraulic conductivity increased over time. For those GCLs that retained low hydraulic conductivity throughout the test, the hydraulic conductivity decreased initially and then remained essentially constant.

Major cation concentrations shown in Fig. 4 are from the test illustrated in Fig. 3. Na^+ concentrations in the effluent decreased rapidly for approximately 40 PVF and then gradually dropped to the influent concentration by approximately 80 PVF, which was due to slow rate-limited cation exchange reaction (Jo et al. 2006). In contrast, the concentrations of Ca^{2+}, Mg^{2+}, and K^+ in the effluent increased over the testing period until reaching the inflow concentration at approximately 80 PVF. These observations indicate that Ca^{2+}, Mg^{2+}, and K^+ replaced Na in the exchange complex of the bentonite. Comparison of Figs. 3 and 4 shows that that hydraulic conductivity and major cations in inflow and effluent

Table 4. Hydraulic Conductivity of GCLs Permeated with RSL, NSL, and DI Water

GCL	Permeant liquid	PVF	Total test time (year)	Termination criteria satisfied?				Hydraulic conductivity (m/s)	K/K_{DI}
				Hydraulic	EC	pH	Major cations		
CS	RSL	208	1.8	Yes	Yes	Yes	Yes	1.9×10^{-10}	8.6
	NSL	239	1.8	Yes	Yes	Yes	Yes	2.8×10^{-10}	12.7
	DI	12.8	0.3	Yes	No	No	No	2.2×10^{-11}	1.0
GS	RSL	188	1.8	Yes	Yes	Yes	Yes	1.7×10^{-10}	20.2
	NSL	198	1.8	Yes	Yes	Yes	Yes	1.3×10^{-10}	15.5
	DI	7.5	0.3	Yes	No	No	No	8.4×10^{-12}	1.0
CPL	RSL	217	1.8	Yes	Yes	Yes	Yes	2.7×10^{-10}	24.5
	NSL	170	1.8	Yes	Yes	Yes	Yes	1.2×10^{-10}	10.9
	DI	11.8	0.8	Yes	No	No	No	1.1×10^{-11}	1.0
GPL1	NSL	74.2	0.9	Yes	Yes	Yes	Yes	9.6×10^{-11}	6.4
	DI	29.8	0.7	Yes	No	No	No	1.5×10^{-11}	1.0
GPL2	RSL	228	1.8	Yes	Yes	Yes	Yes	5.6×10^{-10}	73.7
	NSL	140	1.8	Yes	Yes	Yes	Yes	7.5×10^{-10}	99.0
	DI	2.9	0.8	Yes	No	No	No	7.6×10^{-12}	1.0
CPH	RSL	21.4	2.4	Yes	No	No	No	3.8×10^{-12}	1.6
	NSL	28.7	2.4	Yes	No	No	No	4.9×10^{-12}	1.5
	DI	12.1	1.7	Yes	No	No	No	3.2×10^{-12}	1.0
GPH	NSL	9.6	0.9	Yes	No	No	No	6.8×10^{-12}	2.4
	DI	1.2	0.4	Yes	No	No	No	3.1×10^{-12}	1.0
BPC	RSL	19.7	2.8	Yes	No	No	No	6.9×10^{-12}	0.4
	NSL	21.2	2.8	Yes	No	No	No	5.1×10^{-12}	0.7
	DI	1.9	0.1	Yes	No	No	No	6.7×10^{-12}	1.0

Note: K = hydraulic conductivity to chemical solution; K_{DI} = hydraulic conductivity to DI water; PVF = pore volume of flow.

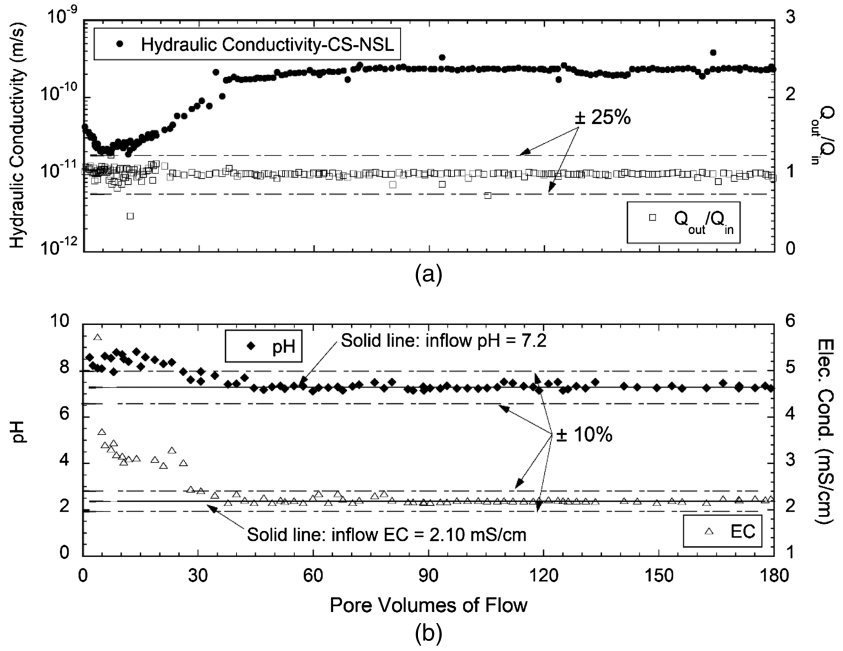

Fig. 3. Hydraulic conductivity, ratio of outflow to inflow, pH, and EC from test on CS GCL using NSL as the permeant liquid

both reach equilibrium at approximately 80 PVF. Similar findings were obtained for all other tests.

Effect of Radionuclides on Hydraulic Conductivity

Hydraulic conductivities of the GCLs exposed to RSL or NSL are compared in Fig. 5. Essentially, the same hydraulic conductivities were obtained using both leachates, with all of the data falling within a band corresponding to a factor of 2, which Daniel et al. (1997) indicate is the reproducibility of hydraulic conductivity tests on GCLs. The similarity in hydraulic conductivities to RSL and NSL reflects the small impact of radionuclides on ionic strength and RMD of RSL (both < 0.03%). Similar swell indices were also obtained with NSL and RSL for each Na-B or B-P GCL (Fig. 6). Based on these findings, RSL and NSL were considered comparable in terms of their effect on hydraulic conductivity of GCLs, and subsequent tests were only conducted with NSL to reduce safety concerns and to simplify disposal of testing waste.

Hydraulic conductivity of the GCLs permeated with RSL or NSL are compared to the hydraulic conductivity to DI water in Fig. 7. Hydraulic conductivities of the CS and GS Na-B GCLs to RSL or NSL are approximately 5–20 times higher than the

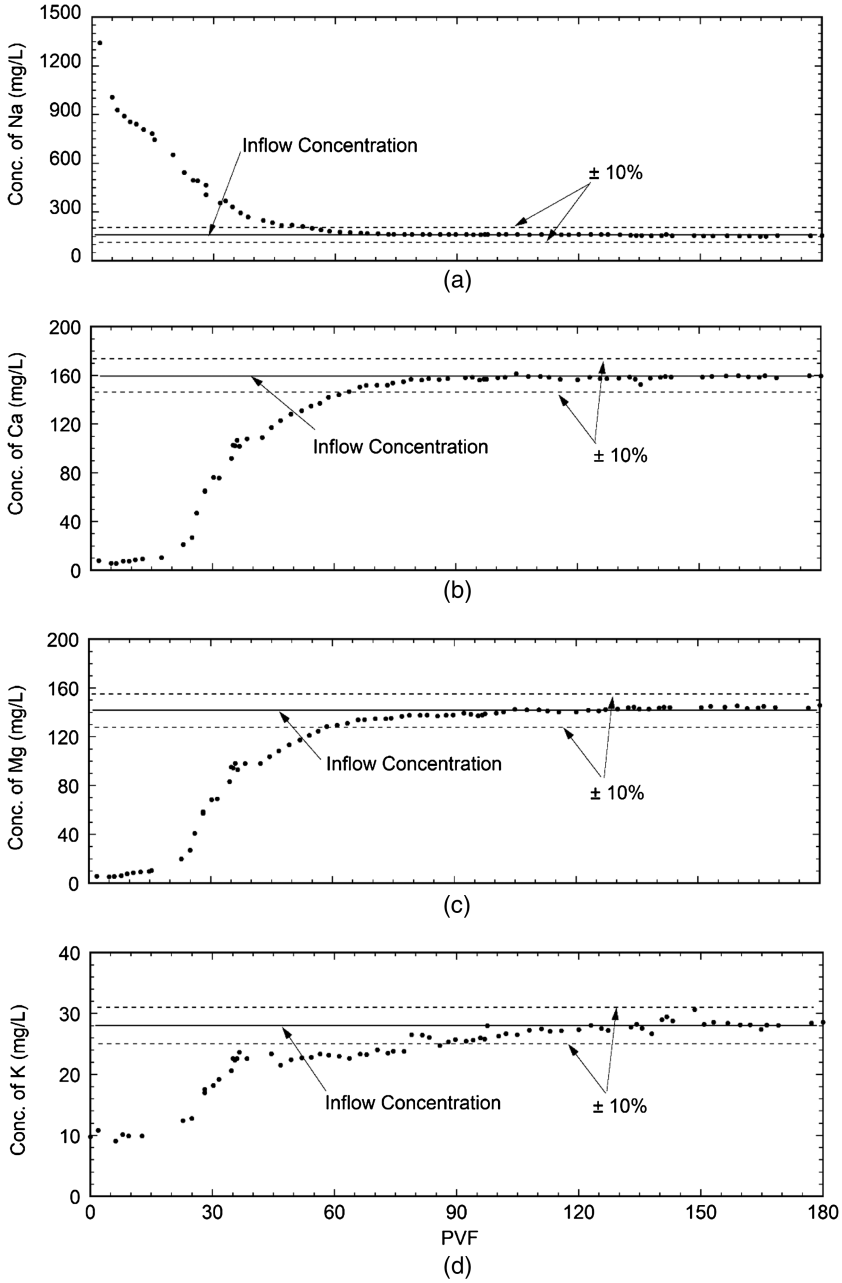

Fig. 4. Concentrations of major cations in influent and effluent for test conducted on CS GCL permeated with NSL: (a) Na^+; (b) Ca^{2+}; (c) Mg^{2+}; (d) K^+

hydraulic conductivity to DI water. Hydraulic conductivity of the B-P GCLs fell into four categories. The GPL2 GCLs were 100 times more permeable to NSL than to DI water, and had the highest hydraulic conductivity of all GCLs in the study. Hydraulic conductivity of the CPL and GPL1 GCLs permeated with RSL or NSL were comparable to conventional GCLs, being approximately 5–25 times more permeable to RSL or NSL than to DI water. The CPH and GPH GCLs had the lowest hydraulic conductivity to RSL or NSL, and had nearly the same hydraulic conductivity as to DI water. The BPC GCL had the lowest hydraulic conductivity of all GCLs ($<10^{-11}$ m/s for NSL, RSL, or DI) and was 1.4–2.5 times less permeable to NSL and RSL than to DI water. Fewer PVF passed through the CPH, GPH, and BPC GCLs than the Na-B GCLs due to the very low flow rate associated with the very low hydraulic conductivity of these GCLs.

Cation Exchange, Swelling, and Hydraulic Conductivity

The RSL and NSL leachates contain divalent cations that have propensity to replace the monovalent Na^+ originally bound to the mineral surface. In NSL and RSL, the total molarity of divalent cations is 30% higher than of monovalent cations, and the total charge associated with the divalent cations is 2.6 times the charge associated with the monovalent cations. Cation exchange is evident in Fig. 4, where Na^+ is eluted due to replacement by Ca^{2+} and Mg^{2+} in the leachate. The exchange complex after testing in the CS, GS, CPL, GPL1, and GPL2 GCLs with NSL or RSL (Table 5) is nearly devoid of monovalent cations, and almost completely comprised of equal amounts of Ca^{2+} and Mg^{2+}. None of polymers in CPL, GPL1, and GPL2 prevented cation exchange. Cation exchange resulted in nearly complete loss in swell by the end of testing, with swell indices ranging between 10 and 12 mL/2 g

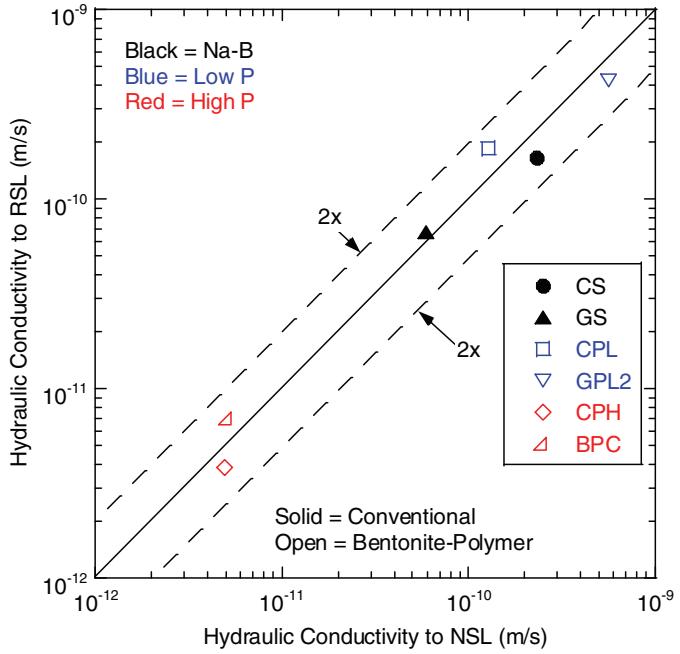

Fig. 5. (Color) Hydraulic conductivity of GCLs to RSL versus hydraulic conductivity to NSL (P = polymer loading)

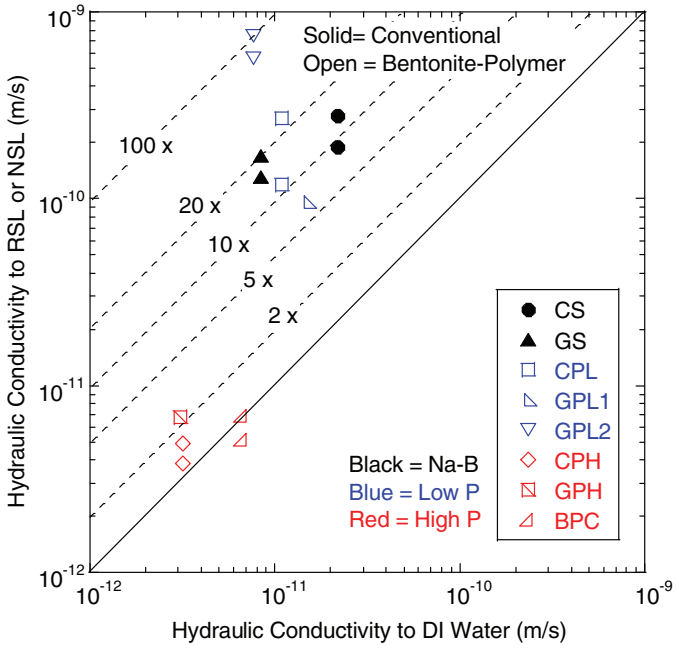

Fig. 7. (Color) Hydraulic conductivity of GCLs to RSL or NSL versus hydraulic conductivity to DI water (P = polymer loading)

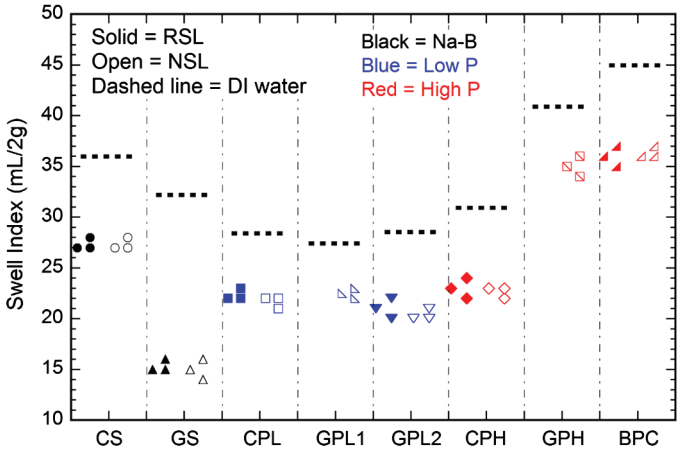

Fig. 6. (Color) Swell index of bentonite from each GCL in RSL, NSL, and DI water (P = polymer loading)

for the CS, GS, CPL, GPL1, and GPL2 GCLs. Prior to permeation, the swell index in leachate ranged between 16 and 27 mL/2 g (average = 22 mL/2 g), and in DI water between 27 and 36 mL/2 g (average = 30 mL/2 g).

Conversion of the Na-B to Ca-Mg-B is responsible for the higher hydraulic conductivity of the conventional Na-B GCLs (CS and GS) to NSL and RSL shown in Fig. 7. The GS Na-B GCL has slightly lower hydraulic conductivity than the CS GCL, despite cation exchange, due to the finer bentonite granule size of bentonite in the GS GCL (Kolstad et al. 2004a).

Polymer Loading

Hydraulic conductivity versus polymer loading is shown in Fig. 8. The B-P GCLs with low–to-modest polymer loading (<5%, CPL, GPL1, and GPL2) have hydraulic conductivity that is 6–99 times higher than the hydraulic conductivity to DI water. In contrast, the B-P GCLs with high polymer loading (≥5%, CPH, GPH, and BPC) all had very low hydraulic conductivity to NSL or RSL, being comparable to the hydraulic conductivity to DI water. This suggests that a threshold in polymer loading exists beyond which the impact of cation exchange on bentonite swell is no longer important, and below which the polymer has insignificant effect on hydraulic conductivity. For the GCLs evaluated in this study, the threshold in polymer loading was approximately 5% (by mass based on LOI), as shown in Fig. 8.

Mechanism Controlling Hydraulic Conductivity of Bentonite–Polymer GCLs to LLW Leachate

The insensitivity of the hydraulic conductivity of the B-P GCLs to swell index suggests that the polymer is controlling the size and shape of the pores rather than swelling of the bentonite. For example, the swell index of Na-B in the CS GCL was higher than the swell index of the B-P in the CPH GCL (Fig. 6), whereas the hydraulic conductivity of CS to RSL and NSL was approximately two orders of magnitude higher than the hydraulic conductivity of CPH GCL permeated with RSL and NSL.

Polymers added to bentonite for hydraulic barrier applications are typically hydrogels, such as Na-carboxymethylcellulose and Na-polyacrylate (Di Emidio et al. 2010; Trauger and Darlington 2000; Kolstad et al. 2004b; Scalia et al. 2014). A hydrogel is a crosslinked polymeric network structure comprised of hydrophilic functional groups that bind water molecules, which results in swelling (De et al. 2002; Soppirnath and Aminabhavi 2002; Ahmed 2015). An image obtained with an optical microscope of B-P from the CPH GCL permeated with DI water is shown in Fig. 9. The liquidlike glutinous hydrogel coats the bentonite particles and binds the particles together.

The hydrogel is believed to function in a manner analogous to bentonite that has undergone osmotic swell, as shown conceptually in Fig. 10. Water molecules in the hydrogel are relatively immobile compared to free water in the pore space, allowing the hydrogel

Table 5. Swell Index and Mole Fractions of Bound Cations in the Exchange Complex of Bentonite in GCLs

GCL	Permeant solution	Swell index in permeant solution (mL/2 g)		Mole fraction of bound cations after termination			
		Before	Termination	Na^+	K^+	Ca^{2+}	Mg^{2+}
CS	RSL	27	11	0.03	0.01	0.47	0.45
	NSL	27	10	0.01	0.02	0.45	0.52
GS	RSL	16	12	0.02	0.01	0.46	0.48
	NSL	16	11	0.04	0.03	0.42	0.49
CPL	RSL	22	10	0.03	0.02	0.43	0.47
	NSL	22	11	0.01	0.02	0.46	0.49
GPL1	NSL	22	10	0.01	0.02	0.41	0.52
GPL2	RSL	20	12	0.02	0.01	0.43	0.47
	NSL	21	10	0.02	0.02	0.40	0.52

Note: Before = bentonite from GCL before permeation; termination = bentonite from GCL after permeating with RSL or NSL. Tests of CPH, GPH, and BPC are still ongoing and therefore analysis has not yet been conducted.

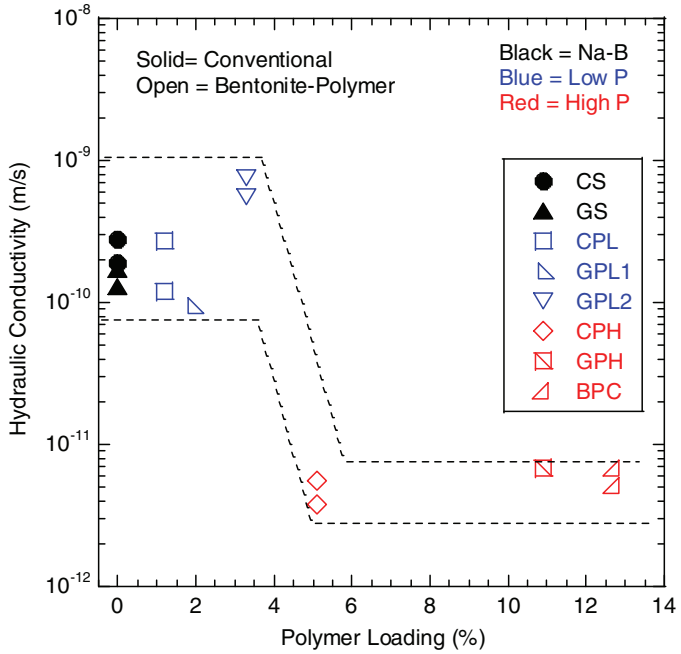

Fig. 8. (Color) Hydraulic conductivity of GCLs as a function of polymer loading (note: conventional GCLs with Na-B have polymer loading = 0%; P = polymer loading)

Fig. 9. (Color) Image of bentonite–polymer from CPH GCL in DI water at 20× using optical microscope; gray matter is hydrated bentonite; clear gel is polymer hydrogel

polymer and water molecules to function hydraulically like a solid [Fig. 10(a)]. Polymer chains and bound water in the hydrogel block larger pores between bentonite granules, forcing water to flow in finer and more tortuous paths within the granules [Fig. 10(b)], resulting in low hydraulic conductivity. In effect, the hydrogel functions analogously to bentonite added to reduce the hydraulic conductivity to water of a more permeable soil, blocking larger pore spaces between particles that would conduct the bulk of flow in soil alone. In contrast to swollen bentonite, however, the hydrogel is a viscous liquidlike gel that is not immobile (Fig. 9), and can migrate when exposed to a hydraulic gradient. Thus, to be effective in blocking flow, the hydrogel must bind to mineral surfaces to limit elution of polymer from the pore space. Moreover, if the polymer loading is insufficient or if the polymer is eluted, not all of the pores will be filled, resulting in larger flow paths and higher hydraulic conductivity [Fig. 10(c)].

To investigate binding between the polymer and bentonite, SEM images were obtained of the CPH GCL permeated with DI water (Fig. 11). The SEM image shows that the polymer forms a three-dimensional net structure in the pores between the bentonite granules. In the saturated system, the polymer net between the granules binds water molecules to form the hydrogel shown in Fig. 9. The edge of an anionic polymer structure may attach to the mineral surface via electrostatic forces associated with cationic bridging, whereas a cationic polymer may bind via electrostatic interactions with the mineral surface (Deng et al. 2006). Edges of the montmorillonite carrying positive charge may also play a role in binding anionic polymers (Black et al. 1965; Heller and Keren 2003).

Visual observation of the effluents from the B-P GCLs indicated that they had significantly higher viscosity and a sticky characteristic, suggesting that polymer was eluted during permeation and that binding between the polymer and mineral was incomplete. Scalia et al. (2014) also report polymer eluting from BPC GCLs permeated with DI water or salt solutions. Anionic polymers, such as polyacrylate and polyacrylamide, that have been used with bentonites can interact with divalent cations (e.g., Ca^{2+}, Mg^{2+}) in the solution, neutralizing charges on the polymer chains (Schweins et al. 2003) that anchor cation bridges to the mineral surface. These hypotheses require further study before definitive conclusions can be made regarding the polymer clogging mechanism.

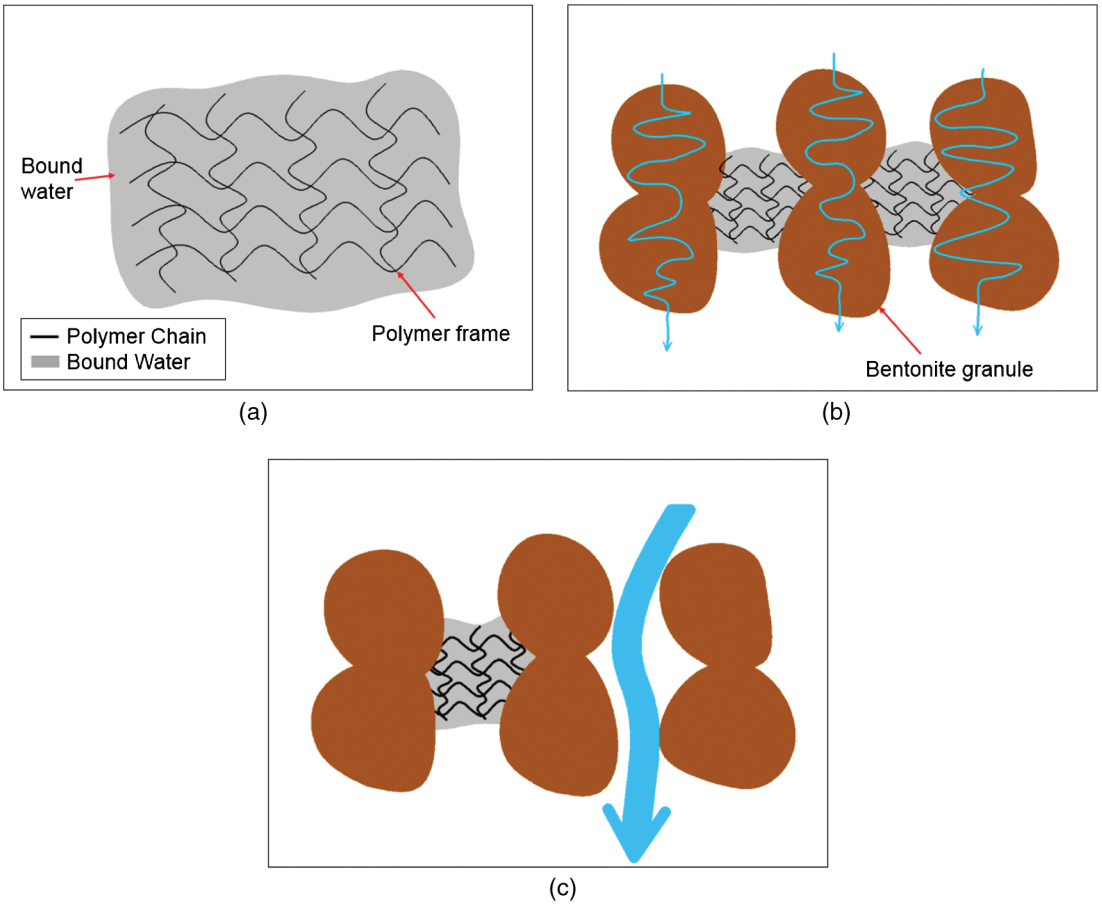

Fig. 10. (Color) Conceptual models for mechanism controlling hydraulic conductivity of bentonite–polymer GCL in LLW leachate: (a) hydrogel with bound water; (b) hydrogel clogs intergranular flow paths and yields low hydraulic conductivity when bentonite granules do not swell and polymer loading is sufficient; (c) insufficient polymer loading in Na-B fails to clog all intergranular flow paths, leaving the unclogged open path controlling the hydraulic conductivity

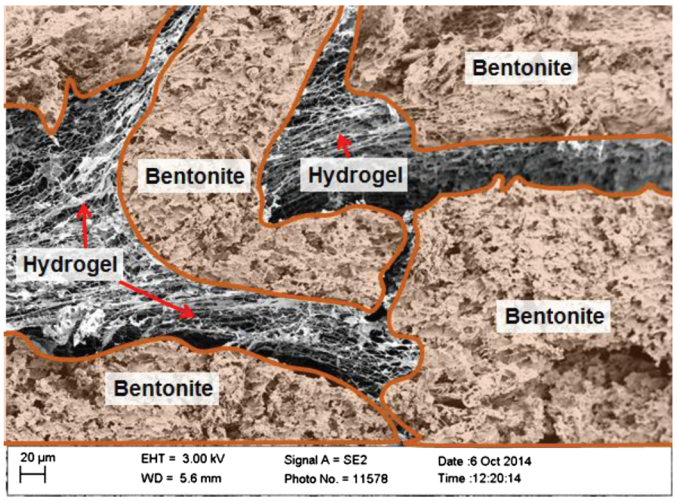

Fig. 11. (Color) SEM image of bentonite–polymer from CPH GCL in DI water after freeze-drying; brown color represents bentonite clusters

The relationship between hydraulic conductivity and polymer loading shown in Fig. 8 also supports the conceptual model of hydrogel clogging pore spaces shown in Fig. 10. The B-P GCLs with low polymer loading (e.g., CPL and GPL1) had high hydraulic conductivity to RSL or NSL, as also observed with the conventional CS and GS GCLs with conventional Na-B, whereas B-P GCLs with high polymer loading (≥5%) had consistently low hydraulic conductivity (Fig. 8). This suggests that sufficient polymer hydrogel is needed to clog the pore spaces in a B-P GCL in the same manner that the hydraulic conductivity of a more permeable soil becomes impermeable to water when a sufficient amount of Na-B is added. Without sufficient polymer hydrogel, a GCL may still have large intergranular pores that control the hydraulic conductivity.

Long-term stability of the hydrogel and its effectiveness in blocking the pore space may be affected by changes in the geochemical conditions over time, as well as by abiotic and biotic degradation processes. A study addressing these issues is currently being conducted.

Summary and Conclusions

A study was conducted to evaluate the hydraulic conductivity of GCLs to leachate characteristic of LLW disposal facilities operated by the U.S. Department of Energy. Two conventional Na-B GCLs and six B-P GCLs were permeated directly with RSL and NSL. Control tests were conducted with DI water. Based on the findings from these tests, the following conclusions were drawn:

1. The effects of NSL and RSL on hydraulic conductivity and swelling of GCLs are not distinguishable due to the small impact of radionuclides on the ionic strength and RMD of RSL

(both < 0.03%). Testing with nonradioactive leachate is recommended to simplify health and safety concerns when investigating GCLs for LLW facilities that have leachate characteristics similar to the leachate evaluated in this study.
2. Conventional CS and GS GCLs containing Na-B can be 10–25 times more permeable to LLW leachate than to the DI water due to suppression of osmotic swelling caused by replacement of native Na^+ in the bentonite with Ca^{2+} and Mg^{2+} in the leachate.
3. B-P GCLs with polymer loading less than 5% by mass as determined by LOI had similar hydraulic conductivity to RSL and NSL as conventional GCLs with Na-B. Without adequate polymer loading, hydrogel formed by hydration of the polymer is unable to clog the pore spaces sufficiently, allowing intergranular channels to control hydraulic conductivity.
4. B-P GCLs with polymer loading exceeding 5% by mass as determined by LOI had hydraulic conductivity to LLW leachate comparable to hydraulic conductivity to DI water. This suggests that a threshold in polymer loading exists beyond which the impact of cation exchange on bentonite swell no longer affects hydraulic conductivity.
5. Clogging of pore spaces between bentonite granules by polymer hydrogel is hypothesized to be responsible for the low hydraulic conductivity of B-P GCLs with higher polymer loading to RSL and NSL. Hydrogels bind water molecules in a three-dimensional structure that clogs pores. Polymer chains in hydrogel carrying negatively charged groups are believed to bind to the mineral surface electrostatically or through cation bridging, retaining the gelatinous polymer within the pore space. These proposed mechanisms need further study before a definitive conclusion can be made regarding their role in controlling the hydraulic conductivity of B-P GCLs.

Acknowledgments

Financial support for this study was provided by the U.S. Department of Energy under Cooperative Agreement Number DE-FC01-06EW07053 (Consortium for Risk Evaluation with Stakeholder Participation III or CRESP). Findings presented in this paper are those of the authors and are not necessarily consistent with policies or opinions of the U.S. Department of Energy.

References

Ahmed, E. (2015). "Hydrogel: Preparation, characterization, and applications: A review." *J. Adv. Res.*, 6(2), 105–121.

Annabi, N., et al. (2010). "Controlling the porosity and microarchitecture of hydrogels for tissue engineering." *Tissue Eng. Part B*, 16(4), 371–383.

Ashmawy, A., Darwish, E., Sotelo, N., and Muhammad, N. (2002). "Hydraulic performance of untreated and polymer-treated bentonite in inorganic landfill leachates." *Clays Clay Miner.*, 50(5), 546–552.

ASTM. (2006a). "Standard specification for reagent water." *ASTM D1193-06*, West Conshohocken, PA.

ASTM. (2006b). "Standard test method for swell index of clay mineral component of geosynthetic clay liners." *ASTM D5890-06*, West Conshohocken, PA.

ASTM. (2007). "Standard test method for particle-size analysis of soils." *ASTM D422-63*, West Conshohocken, PA.

ASTM. (2010). "Standard test method for measuring the exchange complex and cation exchange capacity of inorganic fine-grained soils." *ASTM D7503-10*, West Conshohocken, PA.

ASTM. (2012). "Standard test method for evaluation of hydraulic properties of geosynthetic clay liners permeated with potentially incompatible aqueous solutions." *ASTM D6766-12*, West Conshohocken, PA.

ASTM. (2013). "Standard test methods for loss on ignition (LOI) of solid combustion residues." *ASTM D7348-13*, West Conshohocken, PA.

Benson, C., Oren, A., and Gates, W. (2010). "Hydraulic conductivity of two geosynthetic clay liners permeated with a hyperalkaline solution." *Geotext. Geomemb.*, 28(2), 206–218.

Black, A., Birkner, F., and Morgan, J. (1965). "Destabilization of dilute clay suspensions with labeled polymers." *J. Am. Water Works Assoc.*, 57(12), 1547–1560.

Bouazza, A., and Bowders, J. (2010). *Geosynthetic clay liners for waste containment facilities*, CRC Press, Leiden, Netherlands.

Bradshaw, S., and Benson, C. (2014). "Effect of municipal solid waste leachate on hydraulic conductivity and exchange complex of geosynthetic clay liners." *J. Geotech. Geoenviron. Eng.*, 10.1061/(ASCE)GT.1943-5606.0001050, 04013038.

Daniel, D., Bowders, J., and Gilbert, R. (1997). "Laboratory hydraulic conductivity testing of GCLs in flexible-wall permeameters." *Testing and acceptance criteria for geosynthetic clay liners, STP 1308*, L. Well, ed., ASTM, West Conshohocken, PA, 208–226.

De, S., Atluri, N., Johnson, B., Crone, W., Beebe, D., and Moore, J. (2002). "Equilibrium swelling and kinetics of pH-responsive hydrogels: Models, experiments, and simulations." *J. Microelectromech. Syst.*, 11(5), 544–555.

Deng, Y., Dixon, J., White, G., Loeppert, R., and Juo, A. (2006). "Bonding between polyacrylamide and smectite." *Colloids Surf.*, 281(1), 82–91.

Di Emidio, G., Van Impe, W., and Mazzieri, F. (2010). "A polymer enhanced clay for impermeable geosynthetic clay liners." *Proc., 6th Int. Conf. on Environmental Geotechnics*, Balkema, Rotterdam, Netherlands, 963–967.

Egloffstein, T. (2002). "Bentonite as sealing material in geosynthetic clay liners—Influence of the electrolytic concentration, the ion exchange and ion exchange with simultaneous partial desiccation on permeability." *Proc., Int. Symp. on Clay Geosynthetic Barriers*, H. Zanzinger, R. Koerner, and E. Gartung, eds., Balkema, Rotterdam, Netherlands, 141–153.

Grim, R. (1968). *Clay mineralogy*, 2nd Ed., McGraw-Hill, New York.

Guyonnet, D., et al. (2009). "Performance-based indicators for controlling geosynthetic clay liners in landfill applications." *Geotext. Geomemb.*, 27(5), 321–331.

Heller, H., and Keren, R. (2003). "Anionic polyacrylamide polymer adsorption by pyrophyllite and montmorillonite." *Clays Clay Miner.*, 51(3), 334–339.

Jo, H., Benson, C., and Edil, T. (2006). "Rate-limited cation exchange in thin bentonite barrier layers." *Can. Geotech. J.*, 43(4), 370–391.

Jo, H., Benson, C., Lee, J., Shackelford, C., and Edil, T. (2005). "Long-term hydraulic conductivity of a non-prehydrated geosynthetic clay liner permeated with inorganic salt solutions." *J. Geotech. Geoenviron. Eng.*, 10.1061/(ASCE)1090-0241(2005)131:4(405), 405–417.

Jo, H., Katsumi, T., Benson, C., and Edil, T. (2001). "Hydraulic conductivity and swelling of non-prehydrated GCLs permeated with single species salt solutions." *J. Geotech. Geoenviron. Eng.*, 10.1061/(ASCE)1090-0241(2001)127:7(557), 557–567.

Katsumi, T., Ishimori, H., Onikata, M., and Fukagawa, R. (2008). "Long-term barrier performance of modified bentonite materials against sodium and calcium permeant solutions." *Geotext. Geomemb.*, 26(1), 14–30.

Kolstad, D., Benson, C., and Edil, T. (2004a). "Hydraulic conductivity and swell of nonprehydrated GCLs permeated with multispecies inorganic solutions." *J. Geotech. Geoenviron. Eng.*, 10.1061/(ASCE)1090-0241(2004)130:12(1236), 1236–1249.

Kolstad, D., Benson, C., Edil, T., and Jo, H. (2004b). "Hydraulic conductivity of a dense prehydrated GCL permeated with aggressive inorganic solutions." *Geosynth. Int.*, 11(3), 233–241.

Lee, J., and Shackelford, C. (2005). "Impact of bentonite quality on hydraulic conductivity of geosynthetic clay liners." *J. Geotech. Geoenviron. Eng.*, 10.1061/(ASCE)1090-0241(2005)131:1(64), 64–77.

Meer, S., and Benson, C. (2007). "Hydraulic conductivity of geosynthetic clay liners exhumed from landfill final covers." *J. Geotech. Geoenviron. Eng.*, 10.1061/(ASCE)1090-0241(2007)133:5(550), 550–563.

Mesri, G., and Olson, R. (1971). "Mechanisms controlling the permeability of clays." *Clays Clay Miner.*, 19(3), 151–158.

Nireesha, G., Divya, L., Sowmya, C., Venkateshan, N., Niranjan Babu, M., and Lavakumar, V. (2013). "Lyophilization/freeze drying—A review." *Int. J. Novel Trends Pharm. Sci.*, 3(4), 2277–2782.

Norrish, K., and Quirk, J. (1954). "Crystalline swelling of montmorillonite, use of electrolytes to control swelling." *Nature*, 173(4397), 255–256.

Onikata, M., Kondo, M., Hayashi, N., and Yamanaka, S. (1999). "Complex formation of cation-exchanged montmorillonites with propylene carbonate: Osmotic swelling in aqueous electrolyte solutions." *Clays Clay Miner.*, 47(5), 672–677.

Onikata, M., Kondo, M., and Kamon, M. (1996). "Development and characterization of a multiswellable bentonite." *Environmental geotechnics*, M. Kamon, ed., Taylor and Francis, Rotterdam, Netherlands, 587–590.

Petrov, R., and Rowe, R. (1997). "Geosynthetic clay liner (GCL)—Chemical compatibility by hydraulic conductivity testing and factors impacting its performance." *Can. Geotech. J.*, 34(6), 863–885.

Powell, J., Abitz, R., Broberg, K., Hertel, W., and Johnston, F. (2011). "Status and performance of the on-site disposal facility, Fernald Preserve, Cincinnati, Ohio." *Proc., Waste Management*, WM Symposia, Phoenix, 11137.

Ruhl, J., and Daniel, D. (1997). "Geosynthetic clay liners permeated with chemical solutions and leachates." *J. Geotech. Geoenviron. Eng.*, 10.1061/(ASCE)1090-0241(1997)123:4(369), 369–381.

Scalia, J., and Benson, C. (2011). "Hydraulic conductivity of geosynthetic clay liners exhumed from landfill final covers with composite barriers." *J. Geotech. Geoenviron. Eng.*, 10.1061/(ASCE)GT.1943-5606.0000407, 1–13.

Scalia, J., Benson, C., Bohnhoff, G., Edil, T., and Shackelford, C. (2014). "Long-term hydraulic conductivity of a bentonite-polymer composite permeated with aggressive inorganic solutions." *J. Geotech. Geoenviron. Eng.*, 10.1061/(ASCE)GT.1943-5606.0001040, 04013025.

Schweins, R., Lindner, P., and Huber, K. (2003). "Calcium induced shrinking of NaPA chains: A SANS investigation of single chain behavior." *Macromolecules*, 36(25), 9564–9573.

Shackelford, C., Benson, C., Katsumi, T., Edil, T., and Lin, L. (2000). "Evaluating the hydraulic conductivity of GCLs permeated with non-standard liquids." *Geotext. Geomemb.*, 18(2–4), 133–161.

Shackelford, C., Sevick, G., and Eykholt, G. (2010). "Hydraulic conductivity of geosynthetic clay liners to tailings impoundment solutions." *Geotext. Geomemb.*, 28(2), 149–162.

Shan, H., and Daniel, D. (1991). "Results of laboratory tests on a geotextile/bentonite liner material." *Proc., Geosynthetics*, Industrial Fabrics Association International, St. Paul, MN, 517–535.

Soppirnath, K., and Aminabhavi, T. (2002). "Water transport and drug release study from cross-linked polyacrylamide grafted guar gum hydrogel microspheres for the controlled release application." *Eur. J. Pharm. Biopharm.*, 53(1), 87–98.

Tian, K. (2012). "Durability of high-density polyethylene geomembrane in low-level radioactive waste leachate." M.S. thesis, Dept. of Civil and Environmental Engineering, Univ. of Wisconsin-Madison, Madison, WI.

Tian, K., and Benson, C. (2014). "Hydraulic conductivity of geosynthetic clay liners exposed to low-level radioactive waste leachate." *Proc., Waste Management*, WM Symposia, Phoenix, 1–15.

Trauger, R., and Darlington, J. (2000). "Next-generation geosynthetic clay liners for improved durability and performance." *TR-220*, Colloid Environmental Technologies, Arlington Heights, IL, 2–14.

U.S. EPA. (2007). "Inductively coupled plasma-atomic emission spectrometry." *6010 C*, Washington, DC.

Vasko, S., Jo, H., Benson, C., Edil, T., and Katsumi, T. (2001). "Hydraulic conductivity of partially prehydrated geosynthetic clay liners permeated with aqueous calcium chloride solutions." *Proc., Geosynthetics* Industrial Fabrics Association International (IFAI), Roseville, MN, 685–699.